energies

MDPI

Article

Modeling and Simulation of a Large-Scale Wind Power Plant Considering Grid Code Requirements

Sinawo Nomandela *, Mkhululi E. S. Mnguni and Atanda K. Raji

Department of Electrical, Electronic and Computer Engineering, Cape Peninsula University of Technology, P.O. Box 1906 Bellville, Cape Town 7353, South Africa; mngunim@cput.ac.za (M.E.S.M.); rajia@cput.ac.za (A.K.R.)
* Correspondence: nomandelas@cput.ac.za

Abstract: The load demand to a power grid, as well as the interest in clean and low-cost energy resources, has led to the high integration of wind power plants into power system grids. There are grid code standards that are set for the design and integration of these wind power plants. These codes often look at the design operation of the wind power plant in islanded mode, where possible analysis of the most sensitive power system quantities such as voltage, frequency, reactive power, etc. is carried out. Therefore, in this study, attention was paid to the application of these codes to keep the design and integration of wind power plants well standardized as much as possible. The purpose of this paper is to review and discuss the literature and theory about the design of wind turbine generators and model and simulate a large-scale wind power plant. The modeling was successfully carried out on RSCAD, and the results obtained show that the wind power plant can be further used for other studies such as voltage stability improvement in power grids.

Keywords: modeling; wind turbine (WT); wind turbine generator unit (WTGU); wind power plant (WPP); wind turbine power coefficient

check for updates

Citation: Nomandela, S.; Mnguni, M.E.S.; Raji, A.K. Modeling and Simulation of a Large-Scale Wind Power Plant Considering Grid Code Requirements. *Energies* **2023**, *16*, 2897. https://doi.org/10.3390/en16062897

Academic Editor: Frede Blaabjerg

Received: 5 March 2023
Revised: 15 March 2023
Accepted: 17 March 2023
Published: 21 March 2023

1. Introduction

Integration of wind power plants (WPPs) is increasing in the last few decades. As a result, the installed capacity in the past ten years has increased from 180 GW to 732 GW in the 2010–2020 period [1,2]. This clearly shows that WPPs will have a higher share of power in modern power grids in the future. The use of large-scale WPPs simulations in the analysis of power system problems requires detailed modeling of all components involved in completing a WPP starting from each wind turbine generator unit (WTGU) up to the transmission line system connecting the entire system into the power grid [3]. Moreover, the renewable energy grid code specifications must be followed when modeling such a system so that the system can be industry relevant [4].

WPPs can be operated either in a grid-connected mode or a standalone mode. Even if the WPP is meant for grid integration, the testing of verification of grid code specifications must be carried out in a standalone mode of operation. However, the research that has been carried out rarely considers the WPPs in an islanded mode of operation. In addition, some of the published work makes use of a single wind turbine generator unit (WTGU) and assumes it is a complete WPP (as it is supposed to consider the modeling of multiple WTGUs to accommodate WPP dynamics at large). Most importantly for scholarly benefits, little work has been carried out covering the theory about wind turbine generator (WTG) operation from the power produced by wind up to the output electrical power.

A study of a WPP integration into a weak distribution network is proposed in [4]. Their WPP model has 6 MW single WTGs large enough to represent a reasonable large-scale WPP. A 9 MW single WTG for the integration into the grid through the static synchronous compensator (STATCOM) is modeled in [5].

It is understood that the computation of each component consumes time. In a wind power plant area, the wind speed is not the same. This means that the power produced by each wind turbine generator differs from one another. However, since there are many turbines in a wind power plant, the dynamic behavior from one individual wind turbine is canceled by the others. Therefore, the results obtained in [5] may not be precise. The same applies to [6]; their model may not bring enough validation for their study. Additionally, none of these models were first run standalone for grid compliance tests (as the grid codes require). For instance, for all of the WPPs that were used in the studies referenced [7–13], none of their models were first simulated and analyzed in standalone mode, which makes it difficult to conclude whether their models comply with the grid code requirements or not. It is again understood that the aim of the study was not to evaluate the standalone operation of the plant. However, validation of the output in a plant is important before it is integrated into the power grid. This violates the design requirements of the wind power plants (WPPs for grid integration as mentioned in [14].

Therefore, the contribution of this research is to provide significant information about WPPs. Also, unlike the existing research, this research includes detailed modeling from scratch using practical data from a wind turbine manufacturer. The WPP modeled in this article is large-scale and is simulated in real-time based on the grid code specifications in terms of voltage and frequency requirements, and therefore accommodates the grid compliance test well.

This article is organized as follows: Following the introduction, Section 2 discusses the wind power plant (WPP) overview. Modeling is discussed in Section 3. The results are produced in Section 4, and their discussions are provided in Section 5. Finally, conclusions are drawn in Section 6.

2. Wind Power Plant Overview

A wind power plant (WPP) is a group of wind turbine generator units (WTGUs) installed in a large land for bulk electrical power generation. A WPP can be operated in two modes depending on the power grid stability requirements. These methods are grid-connected and standalone (islanded) modes. In grid-connected mode, a WPP contributes additional power when the load demand in the grid has increased. In standalone mode, it serves as an emergency supply for individual loads when the power supplied by the grid is insufficient [15–17].

WPPs are installed in windy sites to ensure maximum power production. The spacing between the WPP WTGUs is ensured to prevent upwind turbines from interfering with the wind received by those located downwind. This is due to the fact that the wind is slowed as some of its energy is extracted by the rotor of WTGU, which reduces the power available to downwind WTGUs. Figure 1 shows the optimum spacing of WTGUs for a WPP [15].

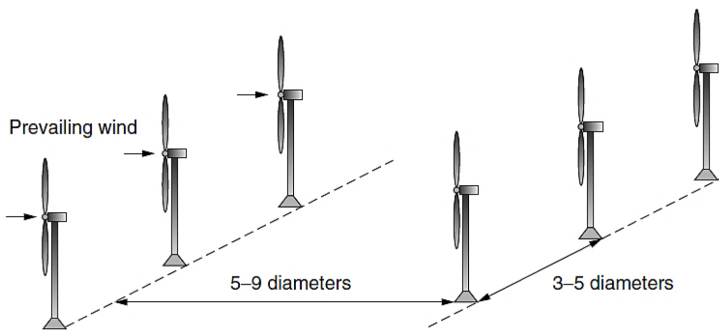

Figure 1. Estimated optimum spacing of towers of three-five rotor diameters between wind turbine generators within a row and 5–9 diameters between rows.

Other important considerations to be made when developing a WPP are as follows [15]:

1. Reduced cost of site development;
2. Simplification of connection to transmission lines;
3. Centralized access for operation and maintenance.

WTGUs are classified by describing them in terms of the axis around which the wind turbine (WT) blades rotate. Most WTGUs are horizontal-axis wind turbines (HAWTs), and some are vertical-axis wind turbines (VAWTs). The HAWTs are either upwind machines or downwind machines.

However, unlike HAWTs, VAWTs accept the wind from any direction, and this forms one of its advantages. The principal advantage of VAWTs is that they do not need any kind of yaw control to keep them facing the wind, and the heavy electrical generator is located on the ground, where it can be serviced easily. Figure 2 shows these types of WTGUs [15].

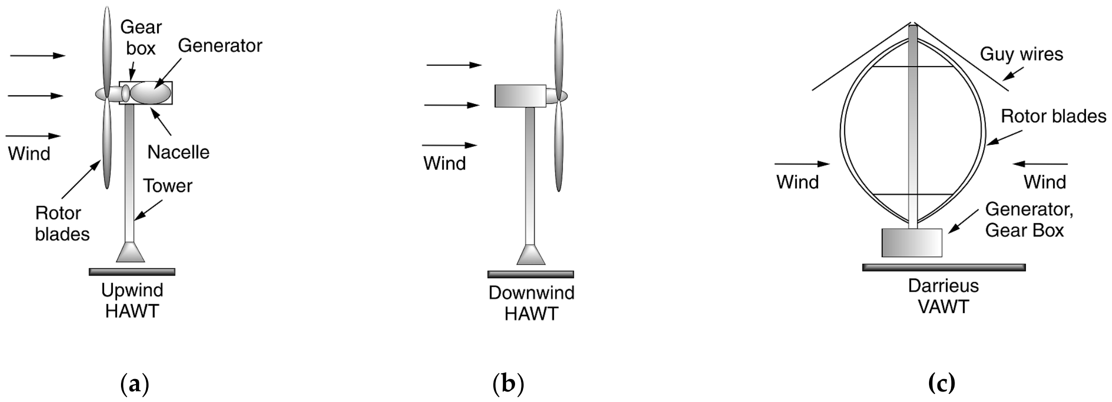

Figure 2. Horizontal axis wind turbines (HAWT): (**a**) upwind HAWT, and (**b**) downwind HAWT. Vertical axis wind turbine (VAWT): (**c**) Darrieus VAWT.

2.1. Wind Turbine Mechanical Power Prediction

The power output of a wind turbine (WT) varies based on wind speed. Every WT has a characteristic power performance curve that is used for the prediction of its output power without taking into consideration the technical details of its components. The power curve gives the output electrical power as a function of the hub height wind speed.

There are three key points of the velocity scale to which the performance of a given wind turbine generator can be related, as described below [15,16].

Cut-in speed. The minimum wind speed at which the machine will deliver useful power. Below this speed, there is no power generated.

Rated wind speed. The wind speed at which the rated power is reached. The rated power is generally the maximum output power of the electrical generator.

Cut-out speed. The maximum wind speed at which the turbine is allowed to deliver power. It is usually limited by engineering design and safety constraints.

Figure 3 is an example of a power curve of a WT [16]. Power curves for existing machines are normally obtained from the WT manufacturers. These curves are derived from the field tests using standardized testing methods.

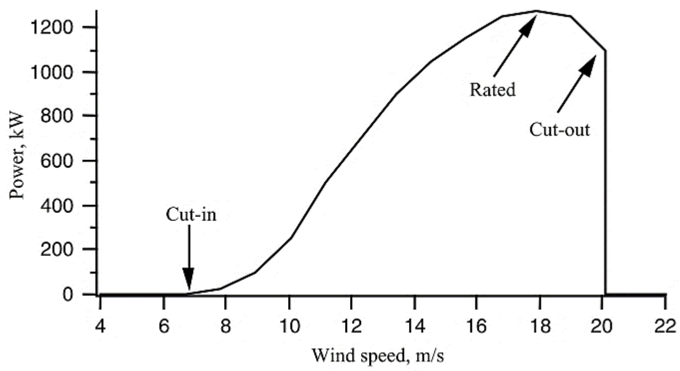

Figure 3. General wind turbine power curve.

2.2. Wind Turbine Generator Unit Electrical Power Production

The available power from the moving wind. The moving wind column consists of mass m in kilograms (kg) and velocity v_w in meters per second (m/s). The moving wind produces kinetic energy k_e in joules (J) and is given by Equation (1).

$$k_e = \frac{1}{2}m{v_w}^2 \tag{1}$$

The mass m is given by Equation (2).

$$m = \rho A v_w t \tag{2}$$

The variables ρ, A, v_w, and t is the density of air in kilograms per cubic meter (kg/m^3), the area swept by the turbine blades in square meters (m^2), the velocity of the wind in meters per second (m/s), and time in seconds (s).

At standard conditions (sea level, 15 °C), the density of air ρ is 1.225 kg/m^3. The area A swept by the turbine blades is given by Equation (3).

$$A = \pi\left(\frac{D}{2}\right)^2 = \pi(R)^2 \tag{3}$$

The symbol D in (3) is the diameter made by the circular movement of the turbines in meters (m), π (Pi) is constant and R is the radius equivalent to the length of the turbine blade. The radius is also in meters (m).

Substituting Equation (3) into Equation (2) results in Equation (4).

$$m = \rho\pi(R)^2 v_w t \tag{4}$$

This leads to the equation of the kinetic energy represented as shown in (5).

$$k_e = \frac{1}{2}\rho\pi(R)^2{v_w}^3 t \tag{5}$$

Power is defined as the rate at which work is carried out. Mathematically, this definition is given by Equation (6).

$$P_W = \frac{k_e}{t} \tag{6}$$

The symbol P_W in (6) is the power in watts (W) produced by the moving air column. Substituting (5) into (6) gives Equation (7).

$$P_W = \frac{1}{2}\rho\pi(R)^2{v_w}^3 \tag{7}$$

The mechanical power produced by the wind turbine shaft. Theoretically, the electrical power extracted by the wind turbine is 59% of the power produced by the wind. This is the principle of Betz and is called the Betz Limit [16]. Practically this limit varies between 40% and 48% [18,19]. That being said, not all of the power produced by the moving air column is converted to electrical power, a certain amount of power is lost due to the wind turbine's efficiency, namely the wind turbine's power coefficient C_p.

The wind turbine power coefficient is also referred to as the wind energy utilization coefficient. The wind energy utilization coefficient is ideally made up of two efficiencies, namely wind turbine efficiency (n_{WT}) and mechanical efficiency or gearbox efficiency (n_G). Figure 4 shows the graphical analysis of results from the Betz Limit [16].

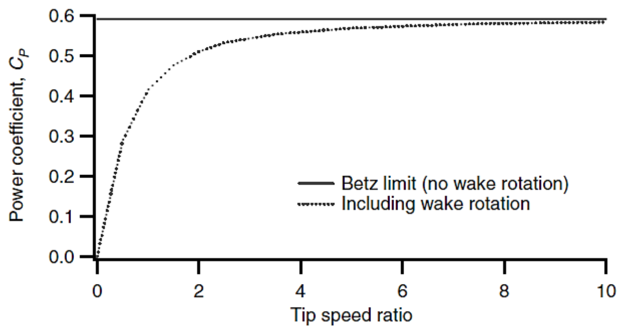

Figure 4. Theoretical maximum power coefficient as a function of tip speed ratio for an ideal horizontal axis wind turbine, with and without wake rotation.

The product of the two aforementioned efficiencies can be used to express C_p as shown in Equation (8).

$$C_p = n_{WTGU} = n_{WT} n_G \tag{8}$$

Since the general definition of efficiency is the percentage ratio of the output power over the input power, C_p can also be called the wind turbine generator unit (WTGU) efficiency n_{WTGU}. For this reason, (8) can also be manipulated to form Equation (9).

$$C_p = n_{WTGU} = \frac{P_{Out}}{P_{In}}(100) \tag{9}$$

The variables P_{Out} and P_{In} in (9) are the output power and input power. Concerning the WTGU, Equation (9) is rewritten in Equation (10).

$$C_p = \frac{P_{WT}}{P_W}(100) \tag{10}$$

In (10), the symbol P_{WT} is the mechanical power produced by the wind turbine shaft from the moving air column, and P_W is the power of the moving air column [20]. The mechanical power of the wind turbine shaft P_{WT} is the same power the electrical generator converts into electrical power, and can therefore still be given a symbol P_{Mech}, the mechanical power of the wind turbine.

From Equation (10), the wind turbine power can be derived by making the wind turbine's mechanical power the subject of the equation as shown in Equation (11).

$$P_{WT} = P_{Mech} = C_p P_W \tag{11}$$

The energy utilization coefficient depends on the design of the wind turbine and the angle at which the wind attacks the turbine blades. The conclusion is drawn from the Betz Limit that the mechanical power extracted by the wind turbine from the moving air column can be given by Equation (12).

$$P_{WT} = P_{Mech} = \frac{1}{2}\rho\pi C_p (R)^2 {v_w}^3 \tag{12}$$

The wind turbine's power coefficient C_p depends on the pitch angle adjustments of the wind turbines.

The mechanical power of the wind turbine shaft to electrical power. A generator is a device that converts mechanical power to electrical power. Many wind turbine generator units (WTGUs) installed in grid-connected applications use a squirrel cage induction generator (SCIG). This type of generator operates within a narrow range of speed slightly higher than its synchronous speed. (A four-pole generator operating in a 50 Hz grid has a synchronous speed of 1500 rpm). The main advantages of a SCIG are that it is rugged, cheap, and easy to connect to an electrical network [16].

The wind turbine shaft is attached to the wind turbine rotor through the hub. The wind turbine shaft is said to be a low-speed shaft since it spins at the same speed (between 7 rpm and 12 rpm ideally) as the wind turbine blades. To produce electrical energy, it is necessary to increase the turning speed of the low-speed shaft to a higher speed, which is required for a generator to produce the rated output power. This is where the gearbox plays a major role in increasing the turning speed of the wind turbine shaft, depending on the ratio of the gearbox. This rotational speed is transferred to the high-speed shaft of the generator, which theoretically rotates from 700 rpm to 1200 rpm [19,21].

3. Modeling

The experiments carried out in this research are conducted using Real-Time Digital Simulator (RTDS) devices. These devices are driven by the software Real-time Computer-Aided Design (RSCAD). RSCAD consists of two modules, the Draft module, and the Runtime module. The draft module is used for modeling, and therefore in this study, it was used for modeling the wind power plant (WPP) and its components. The Runtime module was used for simulation, whose computation is run on the RTDS devices.

The modeling of a WPP is described in this section, starting from the parameters used for a WPP in Section 3.1. In Section 3.2, the wind turbine model is also described, as well as how it was modeled, followed by the induction generator model in Section 3.3. Moreover, the modeling of a WPP high-voltage transformer, WPP high-voltage transmission line, and the WPP receiving-end reactive power compensating device is carried out in Sections 3.4–3.6.

3.1. Parameters

3.1.1. Wind Turbine Parameters

The wind turbine parameters used in the study were obtained from the Vestas brochure by the title 4 MW Wind Platform, and are listed in Tables 1 and 2 below.

Table 1. Vestas V117-4.2 MW wind turbine and rotor data.

Parameter	Values
Rotor diameter (D_R)	117 m
Swept area (A_S)	10.751 m^2
Minimum turbine angular speed, ω_{TRMin}	2.1 rpm = 0.22 rad/s
Nominal turbine angular speed, ω_{TRN}	9.9 rpm = 1.035 rad/s
Maximum turbine angular speed, ω_{TRMax}	17.7 rpm = 1.85 rad/s

Table 2. Vestas V117-4.2 MW wind turbine operating data.

Parameter	Values
Nominal power (P_N)	4 MW/4.2 MW
Cut-in-speed (v_{CI})	3 m/s
Nominal speed (v_N)	14 m/s
Cut-out-speed (v_{CO})	25 m/s
Re-cut-in-speed (V_{R-CI})	23 m/s
Wind class	EC IB-T/IEC IIA-T/IEC S-T
Standard operating temperatures	−20 °C to 45 °C with de-rating above 30 °C at 4 MW
Nominal power (P_N)	4 MW/4.2 MW
Cut-in-speed (v_{CI})	3 m/s
Nominal speed (v_N)	14 m/s

3.1.2. Induction Generator Parameters

The squirrel-cage induction generator parameters were also used in this research, and were obtained from Appendix B Generator Parameters of the book Power Conversion and Control of Wind Energy Systems, and are listed in Table 3 below.

Table 3. Squirrel-cage induction generator parameters.

Parameter	Actual Values	Per Unit Values
Rated output power	4.0 MW	-
Rated mechanical power	4.0606 MW	
Rated apparent power	4.842 MVA	
Rated line-to-line voltage	4000 V (RMS)	
Rated phase voltage = Base voltage	2309.4 V (RMS)	
Rated stator current = Base current	698.88 A (RMS)	
Rated stator frequency	50 Hz	
Rated power factor	0.8261	
Rated rotor speed	1510.5 rpm	
Rated mechanical torque	25.671 kN·m	
Rated stator flux linkage	7.3917 Wb (RMS)	
Rated rotor flux linkage	6.7114 Wb (RMS)	
Stator winding resistance	22.104 mΩ	0.0067
Rotor winding resistance	23.1515 mΩ	0.0069
Stator leakage inductance	1.698 mH	
Stator leakage reactance	j0.53344 Ω	j0.1615
Rotor leakage inductance	1.698 mH	
Rotor leakage reactance	j0.53344 Ω	j0.1615
Magnetizing inductance	33.597 mH	
Magnetizing reactance	j10.5548 Ω	j3.1946
Base flux linkage	7.3511 Wb (RMS)	
Base impedance	3.3044 Ω	
Base inductance	10.518 mH	
Base capacitance	963.29 uF	

The letter j represents the reactance values of the machine.

3.2. Wind Turbine Model

The wind turbine selected for this study is the upwind horizontal axis (HAWT) since it is the most manufactured and installed in the industry. This wind turbine is modeled on the RSCAD and the Vestas V117-4.2 MW wind turbine parameters were used. Figure 5 shows the wind turbine model on the RSCAD draft.

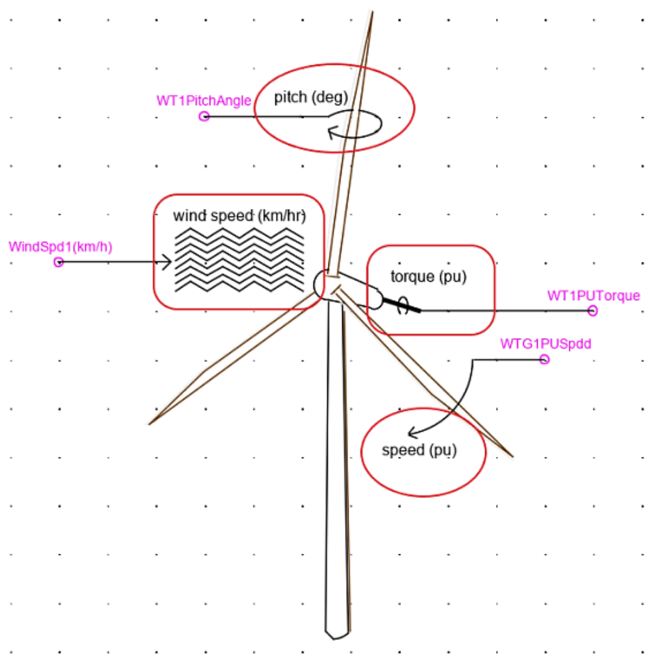

Figure 5. Upwind horizontal axis wind turbine, Vestas V117-4.2 MW.

3.2.1. Wind Turbine Modeling

The wind turbine model in the above figure has three input signals written pitch (deg), wind speed (km/h), and speed (pu) shown in the red zones. To get this wind turbine model working, parameters need to be set and the mapping of control and calculation logic for these input signals is required. In this part, the setting of wind turbine generator parameters, modeling of control, and calculation logic are carried out. Once these control and calculation logics are modeled, an output signal with the name torque (pu) is then coupled to a generator for the conversion of mechanical power to electrical power.

The three inputs and one output, pitch (deg), wind speed (km/h) and speed (pu), and torque (pu) were defined as shown in Figure 5. The signal names WindSpd1(km/h) and WT1PitchAngle are input signals from the wind speed and pitch angle adjustment component. WTG1PUSpdd is the feedback per unit speed signal from the driven generator. WT1PUTorque is the output per unit torque. This signal drives the generator coupled to the wind turbine.

Wind turbines convert about 40% up to 48% of the power produced by the moving wind and transfer it to the generator rotor through the torque mechanism, wherein the later stage is converted to electrical power.

The percentage values stated above represent the efficiency of the wind turbine, which is referred to as the turbine's power coefficient (C_p).

Various equations exist for this parameter. However, the wind power plant model for this study is based on the equation

$$C_p = k_1\left(\lambda + k_2\beta^2 + k_3\right)e^{k_4\lambda} \quad (13)$$

where β and λ are the pitch angle adjustment of the wind turbine blades and the tip speed ratio of the wind turbine.

The tip speed ratio (λ) is given by the following equation

$$\lambda = \frac{v_W}{\omega_{TR}} \quad (14)$$

In the equation, v_W and ω_{TR} are the velocity of wind in meters per second (m/s) and rotational velocity of the turbine rotor in radians per second (rad/s), respectively.

The constants in Equation (13) have the values, $k_1 = -0.5$, $k_2 = -0.022$, $k_3 = -5.6$ and $k_4 = -0.17$. Figure 6 shows the C_p setting values for the constants, k_1, k_2, k_3 and k_4 considered for all of the wind turbine models used in this paper. The literature exists with different equations for the design of wind turbine efficiency (C_p). However, for this paper, we considered Equation (13) due to some difficulties we would experience in RSCAD to define several constants specified for some of the equations.

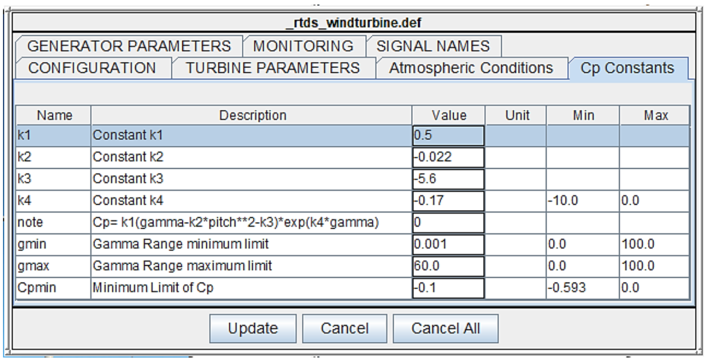

Name	Description	Value	Unit	Min	Max
k1	Constant k1	0.5			
k2	Constant k2	-0.022			
k3	Constant k3	-5.6			
k4	Constant k4	-0.17		-10.0	0.0
note	Cp= k1(gamma-k2*pitch**2-k3)*exp(k4*gamma)	0			
gmin	Gamma Range minimum limit	0.001		0.0	100.0
gmax	Gamma Range maximum limit	60.0		0.0	100.0
Cpmin	Minimum Limit of Cp	-0.1		-0.593	0.0

Figure 6. Power coefficient (*Cp*) parameter settings of the wind turbine. The stars ($*$ and $**$) in the description $\mathrm{C_p} = \mathrm{k1(gamma - k2^*pitch^{**}2 - k3)^*\, exp(k4{*}gamma)}$ presents a multiplication sign and a squared (to the power 2) sign.

The wind turbine operating characteristic exists, formed by plotting the corresponding C_p points versus the wind speed. These curves also depend on the value of the pitch angle. To plot the C_p versus *Wind Speed* (v_w) characteristic curve, the study makes use of at least five-pitch angle adjustments, namely. $\beta 1 = 0°$, $\beta 2 = 5°$, $\beta 3 = 10°$, $\beta 4 = 20°$ and $\beta 5 = 32°$. These values are selected since they are common in the literature, and they justify the relationship between the two variables, C_p and v_w.

3.2.2. Gearbox Modeling

The wind turbine generator model in this study has a turbine rotor rotational speed of 9.9 rpm at nominal, and the induction generator shaft requires thousands of rpms to produce a reasonable amount of power.

A gearbox ratio was calculated by using the nominal values of the wind turbine and the generator rotor speed. At a nominal wind speed of 14 m/s, the wind turbine hub rotational speed is 9.9 rpm while the rated rotor speed of the induction generator is 1510.5 rpm. The generator's rated output power is produced at the rated speed. The gearbox ratio is determined by the equation

$$\omega_{GR} = G\omega_{TR} \tag{15}$$

In the equation, G is the gearbox ratio, ω_{GR} and ω_{TR} are the rated angular rotor speed of the generator's rotor and the wind turbine.

To calculate the value of the gearbox ratio, G was made the subject of the above equation as follows:

$$G = \frac{\omega_{GR}}{\omega_{TR}} \tag{16}$$

The nominal speed values for both the wind turbine hub and the induction generator are substituted as follows

$$G = \frac{1\,510.5 \text{ rpm}}{9.9 \text{ rpm}}$$

$$G = \frac{50.35\pi \text{ rad/s}}{1.036705 \text{ rad/s}}$$

$$G = 152.5757576$$

We also used another method to calculate the gearbox ratio by looking at the amount of torque required by the generator, in comparison with the one produced by the turbine. The mechanical torque equation of the wind turbine is written as

$$T_T = \frac{P_T}{\omega_{TR}} \tag{17}$$

In the equation, T_T and P_T are the mechanical torque in Newton-meters (N·m), and power in Megawatts (MW), produced by the wind turbine.

The amount of torque required by the generator to produce the nominal power of 4 MW is 25.671 kN·m and the torque produced by the wind turbine is calculated as follows.

$$T_T = \frac{4 \text{ MW}}{1.036705 \text{ rad/s}}$$

$$T_T = 3.858378 \text{ MN·m}$$

The mechanical torque transfer calculation was carried out through the gearbox of the wind turbine using the principle defined by the equation

$$T_G = \frac{T_T}{G} \tag{18}$$

In the above equation, T_G is the generator torque. Also, G is made the subject of the formula and the following equation is obtained

$$G = \frac{T_T}{T_G} \tag{19}$$

The values, 3.858378 MN·m, and 25.671 kN·m were then substituted in the variables, T_T and T_G as follows

$$G = \frac{3.858378 \text{ MN·m}}{25.671 \text{ kN·m}}$$

$$G = 152.5757576$$

Figure 7 shows the gearbox ratio and the turbine rotor radius parameter settings.

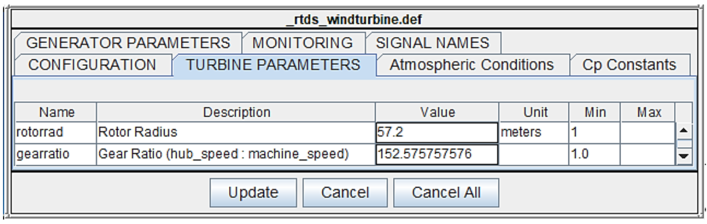

Figure 7. Wind turbine rotor radius and gearbox ratio parameter settings.

In addition to the wind turbine gearbox parameter settings and the rotor radius, the rated MVA, rated frequency, as well as the rated rpm of the generator coupled to the wind turbine, are set as shown in Figure 8.

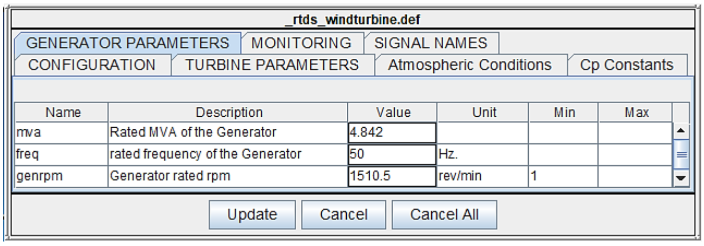

Figure 8. Wind turbine generator-rated apparent power (MVA), frequency, and rotor speed (rpm).

The standard operating temperature range for the wind turbine considered for this paper is −20 °C to 45 °C. A decision is made on the default temperature value of 25 °C, where the wind turbine is assumed to be producing a nominal power of 4/4.2 MW. The default setting value is shown in Figure 9, with that of the default barometric pressure and the percentage humidity.

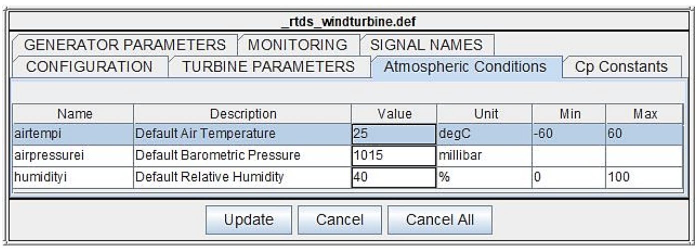

Figure 9. Setting values for the default air temperature, barometric pressure, and relativity.

Certain quantities are monitored and their availability on runtime depends on the settings carried out during the modeling. The part below presents the modeling for wind turbine control, monitoring, and calculation logic.

3.2.3. Control, Monitoring, and Calculation Logic for Wind Turbine

The wind turbine model produces the output per unit torque or high-speed rotation based on the two principal input signals, the pitch angle control adjustment, and wind speed. The control logic for these inputs is shown in Figure 10.

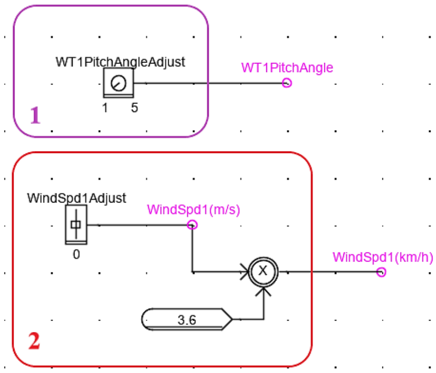

Figure 10. Wind turbine generator blades pitch angle and wind speed adjustment and calculation logic.

The wind speed range specified in the given wind turbine specifications is in meters per second (m/s) and the wind speed input signal to the turbine model provided is required in kilometers per hour (km/h). It is more precise to monitor and tune the wind speed in meters per second. A logic is developed, and its adjustments are in m/s while the output is in units (km/h) required by the wind turbine. The equation is derived for this function and is shown below.

$$x = 3.6(v_W) \quad (20)$$

In the equation, x represents the wind speed in km/h and v_W is the wind speed in m/s. The component with X is the multiplier, and the component labeled WindSpd1Adjust is the slider for tuning the wind speed range.

An output from the slider is labeled WindSpd1(m/s) and it multiplies with the constant number 3.6 as shown in Figure 10. The output labeled WindSpd1(km/h) is a signal name that signally connects the output of the logic to the wind speed input on the wind turbine. Also, in the same figure, Zone 1 shows the dial selector switch for the selection of the angle at which the turbine blades are facing the wind, with its output signal name WT1PitchAngle. The logic to perform this calculation is shown in Zone 2 of Figure 10.

Since the wind speed range is specified from 3 m/s up to 25 m/s, the slider is set such that the adjustment is made from 0 m/s up to 50 m/s for evaluation purposes. The input parameter settings for the WindSpd1Adjust slider are shown in Figure 11.

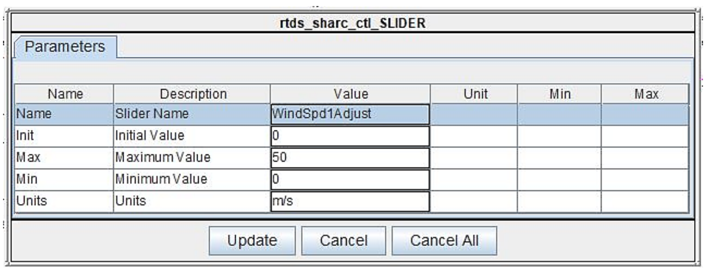
rtds_sharc_ctl_SLIDER

Parameters

Name	Description	Value	Unit	Min	Max
Name	Slider Name	WindSpd1Adjust			
Init	Initial Value	0			
Max	Maximum Value	50			
Min	Minimum Value	0			
Units	Units	m/s			

Update Cancel Cancel All

Figure 11. Wind speed adjustment settings.

The pitch angle adjustment of a wind turbine is not as simple as just punching values in degrees (of rotation). Various parameters are put into consideration in modeling a controller for this feature. As a result of the time that would be spent in designing a controller for this purpose, as well as the theory to be undergone for more understanding about controllers, the study uses a dial selector switch for this feature, whose application does not affect the emphasis of the study. The dial selector switch configuration settings are shown in Figure 12.

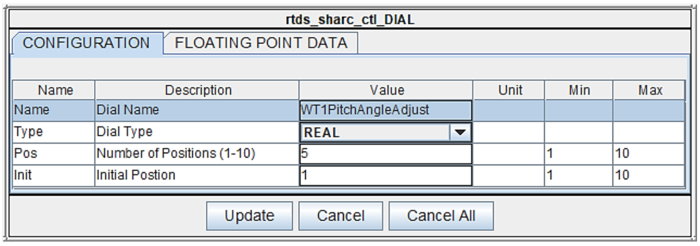

Figure 12. Wind turbine blade pitch angle adjustment slider settings.

In the figure above, the number of positions is set to 5, each position specifying the value of the pitch angle (β), and the settings for these positions are shown in Figure 13.

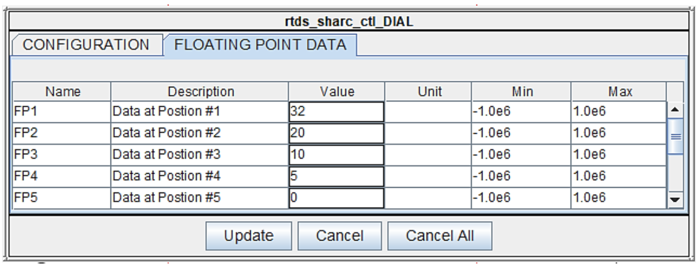

Figure 13. Settings for slider pitch angle values in degrees of rotation.

The wind speed operating range of the Vestas V117-4.2 MW wind turbine is specified from 3 m/s to 25 m/s. Also, the rotational (angular) speed of the turbine rotor is specified in correspondence to the wind speed range and the data is shown in Table 4.

Table 4. Wind speed and angular speed of the wind turbine rotor.

Wind Speed	Wind Turbine Rotor Angular Speed (rpm)	Wind Turbine Rotor Angular Speed (rad/s)
3	2.1	0.219911
14	9.9	1.036705
23	-	-
25	17.6	1.843068

Since the tip speed ratio is calculated from a rad/s value, the turbine rotor speed was converted from rpm to a rad/s unit and the values are shown in the third column in the table above. Two parameters influence turbine efficiency (C_p), β and λ.

The C_p values are determined for each tip speed ratio with different pitch angle adjustments and the results are shown in Table 5.

Table 5. Wind speed and angular speed of the wind turbine rotor based on the 32 degrees pitch angle adjustment.

V_W	C_p	ω_H	λ	β
3	0.405892	0.219911	13	0
14	0.375725	1.036705	13	5
25	0.285222	1.843068	13	10
36	−0.07679	2.666666	13	20
47	−0.82978	3.48	13	32

The value of the tip speed ratio (λ) is constant since the relationship between the increase in wind speed is directly proportional to the increase in the angular speed of the turbine rotor. The turbine coefficient (C_p) versus wind speed curve is plotted for this wind turbine and is shown in Figure 14. This curve is plotted using different values of β and λ. The graph obtained in the plot shows the maximum value of C_p at 0° and it follows the same characteristics as the literature.

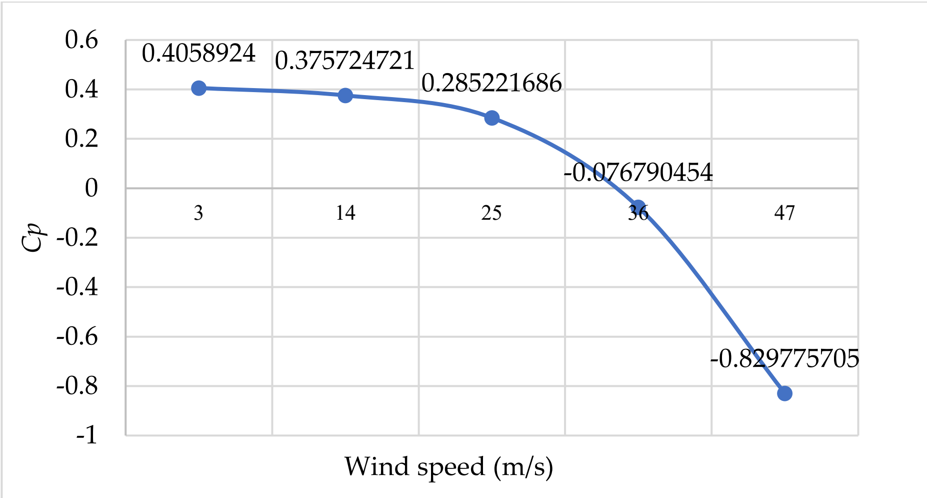

Figure 14. Turbine power coefficient versus the wind speed at different pitch angle adjustments.

The pitch angle controller controls the value of C_p to produce the rated power at multiple ranges of wind speed. When the wind speed is increasing and the pitch angle is 0.4, the power produced by the wind turbine will be a huge amount. Tuning the value of C_p to a lesser value will reduce the power output of the wind turbine. Also, when the wind speed is less, the power will be less, therefore tuning C_p to a higher value increase the power output of the wind turbine. However, the C_p versus the wind speed characteristic for a wind power plant presented in this paper may not be the same as the one found in the literature. This is due to the absence of the pitch angle controller. Besides, the pitch angle controller does not affect the desired output power from the model.

3.3. Induction Generator Model

The power measured from the output of the wind turbine is mechanical and is transferred in the form of a per-unit mechanical torque to the generator it is coupled with. The generator selected for this study is a squirrel-cage induction generator for its simplicity and low-costs. Figure 15 shows the induction generator model.

The induction generator model in the figure has three input signals written and shown in Zone 1, Zone 2, and Zone 3 as PU SPEED INPUT, MODE INPUT, and PU TMECH INPUT. The two input signals are shown in Zone 1 and Zone 3; one is used, depending on the selected input signal which is controlled by the input signal in Zone 2, which is the MODE input signal.

The mode of operation of the induction generator is discussed in the following parts during the modeling of controls, calculation, and monitoring logic. The circuit shown in Zone 5 of Figure 15 is the exciter circuit and is connected to the stator terminals of the induction generator represented by a node in Zone 4, where the signals WTG1TermVR, WTG1TermVY, and WTG1TermVB in the zone are wind turbine's squirrel-cage induction generator stator terminal voltage signals for phases R, Y, and B. This circuit assists in the building up of the induction generator's stator terminal output voltage.

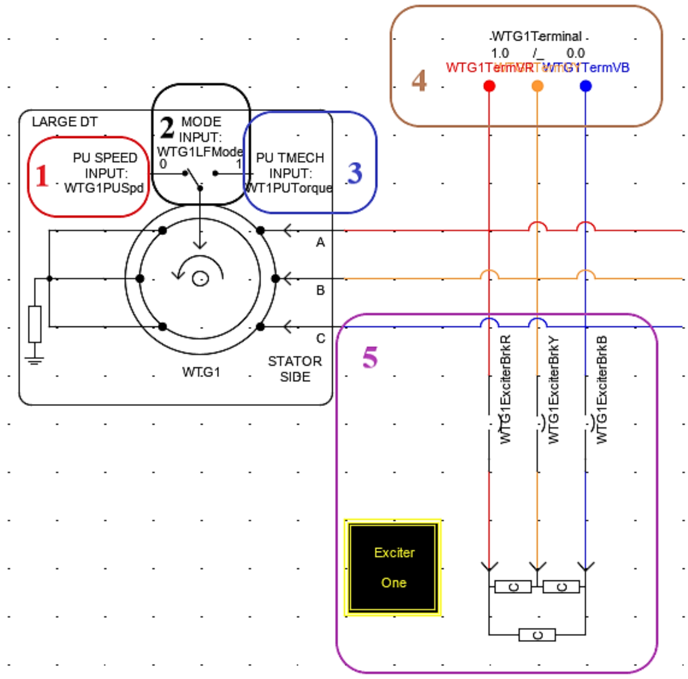

Figure 15. The squirrel-cage induction generator model with the exciter circuit.

To ensure the operation of the induction generator model, some parameters must be defined, as well as the mapping of control and calculation logic for these input signals.

3.3.1. Squirrel-Cage Induction Generator Modeling

One of the most important settings in induction generator modeling is that of defining the motor's electrical parameters as shown in Figure 16.

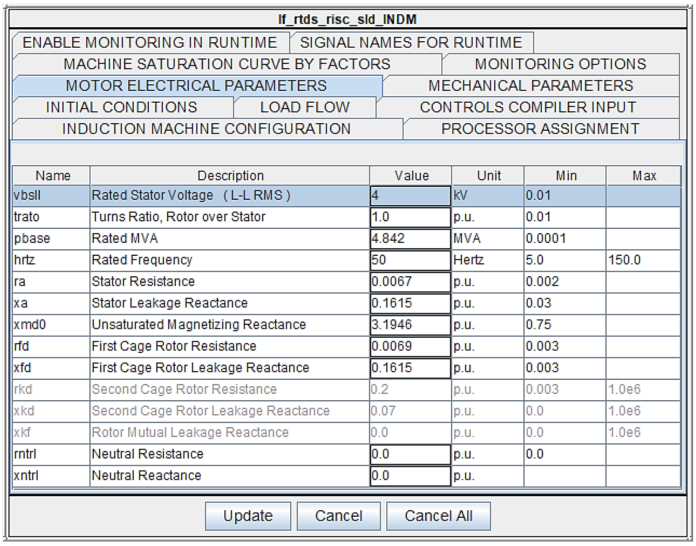

Name	Description	Value	Unit	Min	Max
vbsll	Rated Stator Voltage (L-L RMS)	4	kV	0.01	
trato	Turns Ratio, Rotor over Stator	1.0	p.u.	0.01	
pbase	Rated MVA	4.842	MVA	0.0001	
hrtz	Rated Frequency	50	Hertz	5.0	150.0
ra	Stator Resistance	0.0067	p.u.	0.002	
xa	Stator Leakage Reactance	0.1615	p.u.	0.03	
xmd0	Unsaturated Magnetizing Reactance	3.1946	p.u.	0.75	
rfd	First Cage Rotor Resistance	0.0069	p.u.	0.003	
xfd	First Cage Rotor Leakage Reactance	0.1615	p.u.	0.003	
rkd	Second Cage Rotor Resistance	0.2	p.u.	0.003	1.0e6
xkd	Second Cage Rotor Leakage Reactance	0.07	p.u.	0.0	1.0e6
xkf	Rotor Mutual Leakage Reactance	0.0	p.u.	0.0	1.0e6
rntrl	Neutral Resistance	0.0	p.u.	0.0	
xntrl	Neutral Reactance	0.0	p.u.		

Figure 16. Squirrel-cage induction generator model electrical parameter settings.

The stator resistance, rotor resistance, core resistance, and reactance parameters of this machine are entered in per-unit values. These values are calculated from the base values specified by the guide for RSCAD induction generator modeling.

The following are base values specified for calculating the per-unit values of the machine:

- Base voltage (V_B): Rated line-to-neutral stator voltage of the generator as the base value for the voltage.
- Power: Rated MVA of the machine is used as the base value for the power
- Base current (I_B): Rated stator current of the machine is used as the base value for the current
- Base impedance (Z_B): The ratio of the base voltage (V_B) over the base current (I_B) is used as the base value for the base impedance.

Another setting is that of the generator's inertia constant. As specified from its units, MWs/MVA, is calculated from the values provided in the generator specifications, and the value is set in the mechanical parameters as shown in Figure 17 of the induction generator parameter settings.

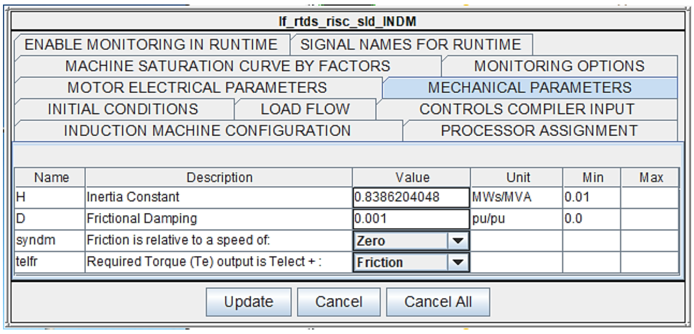

Figure 17. Squirrel-cage induction generator model mechanical parameter settings.

The induction generator produces electric power by converting the mechanical power input to its shaft. The voltage at the generator's stator terminal will never build up even if the torque from the prime mover is enough. For a voltage build-up on the stator terminals of the induction generator, an exciting circuit is required. This circuit produces the voltage from the small amount of current available at the stator terminals during the rotation of the generator's rotor.

3.3.2. Design and Modeling of Squirrel-Cage Induction Generator Excitation Circuit

The SCIG's rated values were used for this calculation. The apparent power (S) was calculated from the rated current and voltage of the induction generator using the equation

$$S = \sqrt{3}IV \tag{21}$$

$$S = \sqrt{3}\ (0.69888\ \text{A})(4\ \text{kV})$$

$$S = 4.84198\ \text{MVA}$$

Induction machines are known as machines that draw a lagging current from the circuit, and their power factor is always assumed to be 0.8 lagging. Therefore, the active power was calculated as

$$P = 4.84198\ \text{MVA}\ (0.8261)$$

$$P = 3.999999\ \text{MW}$$

The total reactive power required from the excitation circuit was calculated using the values of the active and apparent power determined above. The equation

$$Q_T = \sqrt{S^2 - P^2} \tag{22}$$

is used.

In the equation, Q_T is the total reactive power of the excitation circuit and is calculated as

$$Q_T = \sqrt{(4.84198\ \text{MVA})^2 - (3.99999\ \text{MW})^2}$$
$$Q_T = 2.72853\ \text{MVAr}$$

The value calculated here is the minimum reactive power required to excite the induction machine to produce a voltage at the stator terminals. For low cost, the combination of the capacitors to produce Q_T is usually connected in a delta connection. In this connection, the capacitive reactance is three times less than the total reactive power of the circuit. Therefore, the value of 0.909510 MVAr is determined for the excitation circuit model presented in this paper. From this, we calculated the current that will flow through each capacitor using the equation

$$I_Q = \frac{Q_P}{V_{Phase}} \tag{23}$$

In the equation, I_Q, Q_P and V_{Phase} are the current flow in the reactive component, the per-phase reactive power of the excitation circuit, and the per-phase voltage. The voltage is equal to the line-to-line voltage due to the connection method of the reactive component. The reactive current is then calculated as

$$I_Q = \frac{0.909510\ \text{MVAr}}{4\ \text{kV}}$$
$$I_Q = 0.22738\ \text{kA}$$

Also, the capacitive reactance of the per-phase capacitor is determined using the equation:

$$X_C = \frac{V}{I_Q} \tag{24}$$

In the equation, X_C is the capacitive reactance for each capacitor and is calculated as

$$X_C = \frac{4\ \text{kV}}{0.22738\ \text{kA}}$$
$$X_C = 17.591697\ \Omega$$

The setting parameters of the reactive power compensator device used in RSCAD are entered in per-phase micro-Farads. The per-phase micro-Farads value for this circuit is determined using the equation below.

$$C_{Phase} = \frac{1}{2\pi f X_C} \tag{25}$$

In the equation, C_{Phase} is the amount of per-phase capacitance required for each capacitor to generate the minimum amount of the per-phase reactive power, f is the rated frequency of the generator. The calculation is carried out as

$$C_{Phase} = \frac{1}{2\pi(50\ \text{Hz})(17.591697)}$$
$$C_{Phase} = 180.94325\ \text{uF}$$

C_{Phase} is the amount of the per-phase capacitance to be connected to the induction generator stator terminals its excitation. Figure 18 shows the parameter settings entered for the excitation circuit used for an induction generator.

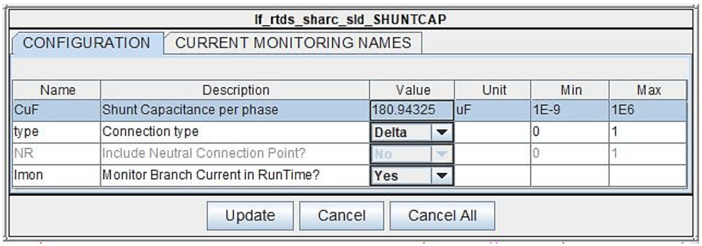

Figure 18. Excitation circuit parameter settings.

In a wind power plant, induction generators are connected in parallel, and the excitation capacitor banks connected to each terminal of a generator make parallel circuits. The capacitor banks, when connected in parallel increase the capacitance in the system. That being said, the value of the capacitance calculated above may vary, depending on the number of wind turbine generators connected to complete the wind power plant.

Therefore, the value of the capacitance for the excitation circuit depends on the connected number of wind turbine generator units. In this paper, we present no fixed value of the capacitance.

3.3.3. Control, Monitoring, and Calculation Logic for Squirrel-Cage Induction Generator

A relationship between wind speed and the turbine rotor speed. The rotor speed increases as the wind speed increases. As a result of this relationship and the per-unit speed control input to the driven generator, a logic is designed, that calculates the per-unit speed from the speed of the wind.

The nominal speed of the wind is 14 m/s, and the wind turbine is expected to be producing a nominal power of 4/4.2 MW at this speed. At 14 m/s of wind speed, the speed input to the generator is expected to be at 1 per unit. The logic was designed as shown in Figure 19.

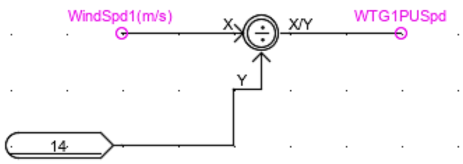

Figure 19. The logic for wind turbine generator per-unit speed control.

In the figure above, constant 14 is the rated wind speed in meters per second (m/s) and is used as the base value for obtaining the per-unit output signal. The designed logic makes use of the calculated per-unit speed of the wind and applies it to the generator.

The component with a division sign produces the output signal assigned WTG1PUSpd. The signal WindSped1 (m/s) is the output from the wind input speed adjusting slider for the wind turbine. The WTG1PUSpd signal is connected to the generator as part of the control signals.

Three signal names were also defined for the control of the induction generator as shown in Figure 20.

The signal name WTG1LFMode controls the mode of operation of the induction generator. When the Lock/Free Switch (WTG1LFSW) is put on Free Mode (OFF state), the generator operates using the input signal WTG1PUTorque and operates through the input signal WTG1PUSpd when the switch is positioned the other way.

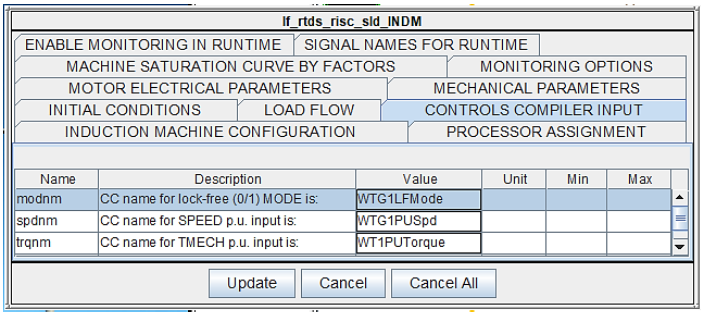

Figure 20. Control's compiler settings for the induction generator model.

Another mapping of signals exists between the wind turbine and the induction generator, namely, the per-unit feedback speed from the induction generator to the wind turbine. Input to the wind turbine this signal is WTG1PUSpdd. This signal is made available by setting parameters to monitor the induction generator as shown in Figure 21.

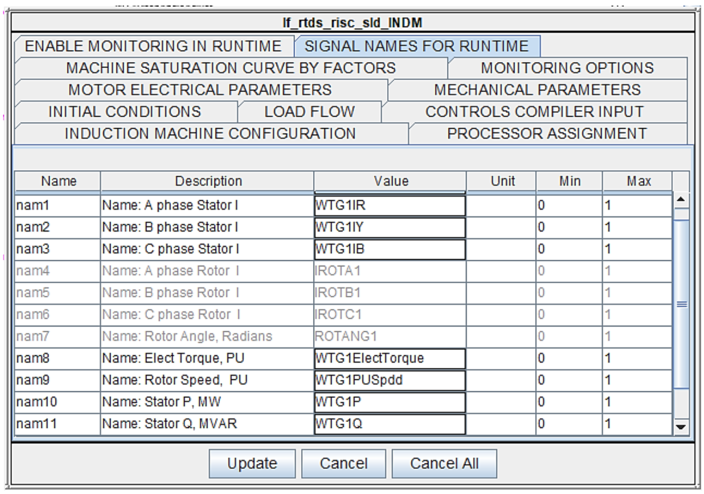

Figure 21. Signal name settings for induction generator model.

Part of the signals monitored in the figure is the stator currents, electrical torque, the rotor speed of the generator, and the output electrical real (P), and reactive (Q) power. Setting these quantities makes them available on the run-time simulation cases for monitoring purposes.

The excitation circuit model for the induction generator model requires control, monitoring, and calculation logic. The logic to perform these functions is shown in Figure 22.

In the figure, Zone 1 shows a switch for controlling the circuit breaker for switching ON/OFF the excitation circuit. Zone 2 shows the logic for calculating and monitoring the reactive power produced by the excitation circuit. This logic determines the reactive power using the product of the RMS current and voltage seen by the circuit. The logic in Zone 3 calculates the RMS voltage from the wind turbine generator (WTG) stator terminals.

The signal names IRYWTG1Eciter, IYBWTG1Eciter, and IBRWTG1Eciter shown in Zone 2 are the phase currents monitored from the exciter circuit. These signals are found in the settings of the capacitor bank model and were set for monitoring as shown in Figure 23.

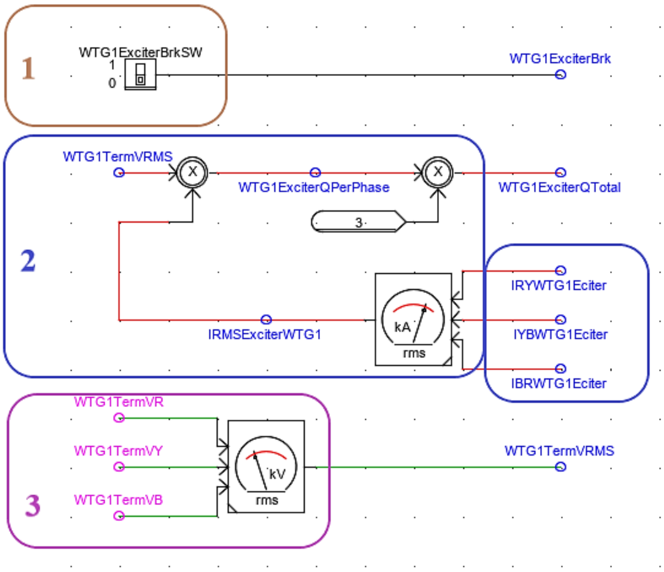

Figure 22. Excitation circuit control, monitoring, and calculation logic.

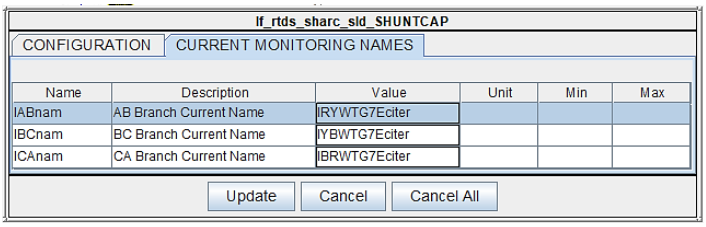
lf_rtds_sharc_sld_SHUNTCAP

CONFIGURATION | CURRENT MONITORING NAMES

Name	Description	Value	Unit	Min	Max
IABnam	AB Branch Current Name	IRYWTG7Eciter			
IBCnam	BC Branch Current Name	IYBWTG7Eciter			
ICAnam	CA Branch Current Name	IBRWTG7Eciter			

Update | Cancel | Cancel All

Figure 23. Induction generator exciter phase current signal settings for the calculation and monitoring of reactive power, exciter current, and voltage.

3.4. Wind Power Plant High-Voltage Transformer Modeling

A complete wind power plant consists of power system components such as generator units, step-up transformers to step up the generated low-voltage to a medium voltage connected to the collector circuit, the medium voltage to high-voltage transformers for stepping up the voltage to a transmission level voltage [22].

The transformers of 5 MVA were selected for each wind turbine generator substation unit (WTGSU). Having looked at the WTGSU transformer capacity of 5 MVA, there are six of these transformers and at full load, each would deliver 5 MVA to the collector busbar. From the collector exists a 24 kV to 230 kV step-up transformer required to deliver eighteen times 5 MVA (equals 90 MVA) to the transmission system through the transmission lines. Therefore, a 90 MVA transformer is selected.

Having modeled all of the major components, each wind turbine generator unit is connected to the collector busbar through WTGSUs (transformers) to complete the collector circuit. Power-generating plants are usually located in remote areas, away from customers. Some literature specifies that one of the advantages pertinent to wind power plants is that they provide clean power closer to the load.

However, depending on the mode of operation the wind power plant is operated, this advantage may not be true for all wind power plants. Power is generated and transmitted to where it is required. To achieve this, a transmission line must be modeled for a wind power plant to make sure that the power reaches the customers even in a remote area. In the case of the transmission system model used for this study, this makes modeling easier as the RSCAD model uses more than one subsystem. To interconnect two or more power system circuits between subsystems, transmission line models are used. The following part presents the transmission line modeling for the wind power plant.

3.5. Wind Power Plant High-Voltage Transmission Line Modeling

RSCAD offers two models of transmission lines, the traveling wave transmission lines and PI section models. Both these models represent transmission lines on the RSCAD. The traveling wave transmission line model is generally preferred only for line models whose length is 15 km and above. Otherwise, the PI section model is used. There are several advantages and disadvantages to these transmission line models. However, for the aim of interconnecting the two systems in this study, the traveling wave transmission line model becomes the best option since it allows the interconnection of two or more subsystems while guaranteeing accuracy. A 15 km transmission line model is used for this model, interconnecting the two systems, the transmission, and the wind power plant system under study.

The parameters used for this transmission line model are obtained from one of the RTDS tutorials, whose data is reliable and does not deviate from the aim of the study. The original line had a length of 100 km and is reduced to 15 km, in the interest of reducing power losses while the purpose of a wind power plant model is kept realistic.

Part of the grid code requirements is that of the frequency, voltage, and reactive power or power factor at the point of common coupling of the wind power plant. The voltage is specified for continuous operation from 0.9 up to 1.0985 per unit for this category. Also, the power factor must be 0.95 and more at the common point of coupling.

The power generated by the wind power plant understudy the minimum power Category C renewable power plants can generate. Also, the reactive power it generates is of a low quantity and therefore is not expected to send it as it is at the receiving end terminal of the transmission system model due to the transmission lines that are rich in the magnetic circuit (which causes a huge absorption of reactive power through the line). For this reason, the same approach of generating and compensating for the reactive power absorbed during the transmission is carried out at the receiving end terminal of the wind power plant transmission line system. Therefore, a wind power plant reactive power-producing device is modeled in the following part.

3.6. Wind Power Plant Receiving-End Reactive Power Compensating Device Modeling

The load demand of 15 MW is considered in this paper. Therefore, the WPP of at least 15 MW is modeled. Corresponding to the active power, the grid codes specify the power factor at the terminals of the Category C renewable power plants at a value of 0.95. The corresponding reactive power for this amount of active power at a power factor of 0.95 is 4.930261578 MVAr.

This is the minimum value of the reactive power compensator device that must be connected at the receiving end terminal of the wind power plant to produce a power factor of 0.95 when the active power produced is 15 MW.

The reactive power compensator device uses capacitor banks. The total capacitance of the capacitor bank is calculated using the equation

$$C_{Total} = \frac{I_Q}{2\pi f V_{Phase}} \tag{26}$$

In the above equation, I_Q and V_{Phase} are the current flow in the reactive component and the per-phase voltage, which is equal to the line-to-line voltage due to the connection method of the reactive component.

The value of I_Q can be found by using the equation below.

$$I_Q = \frac{Q_{Phase}}{V_{Phase}} \tag{27}$$

In the above equation, Q_{Phase} is the per-phase reactance of the capacitor bank.

The value of the current is then calculated as

$$I_Q = \frac{1.643420526\ \text{MVAr}}{0.9(230\ \text{kV})}$$

$$I_Q = 0.07939229594\ \text{kA}$$

Therefore,

$$C_{Phase} = \frac{0.07939229594\ \text{kA}}{2\pi(50\ \text{Hz})(0.9\ \text{PU})(230\ \text{kV})} \quad (28)$$

$$C_{Phase} = 0.1220838294\ \mu\text{F} \quad (29)$$

Capacitor banks cause a lot of transient currents in the power system, which might affect other power system components. The transients are reduced by sequential switching. In the case of sequential switching, capacitor banks are divided into units and this becomes very effective in reducing the transients.

For the capacitor bank presented above, a decision is taken, that there are fourteen units. Therefore, each unit is fourteen times less than 0.1220838294 μF, which then gives a 0.00872035286 μF capacitor bank. The settings parameter for each capacitor is shown in Figure 24.

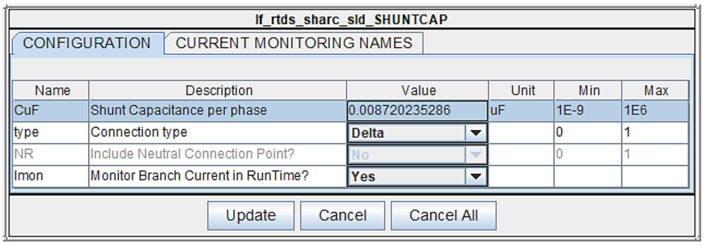

lf_rtds_sharc_sld_SHUNTCAP

CONFIGURATION | CURRENT MONITORING NAMES

Name	Description	Value	Unit	Min	Max
CuF	Shunt Capacitance per phase	0.008720235286	uF	1E-9	1E6
type	Connection type	Delta		0	1
NR	Include Neutral Connection Point?	No		0	1
Imon	Monitor Branch Current in RunTime?	Yes			

Update | Cancel | Cancel All

Figure 24. WPP terminal reactive power compensator device model settings parameters.

Only one unit is shown in this part, though all other units have the same settings menu, with different labeling of signals.

Monitoring is also a requirement for a reactive power compensator. A relationship exists between the current, voltage, and the reactive power produced by the capacitor bank. Using this relationship, the total reactive power contribution can be monitored at the busbar where these capacitor bank units are connected. The logic is shown in Figure 25.

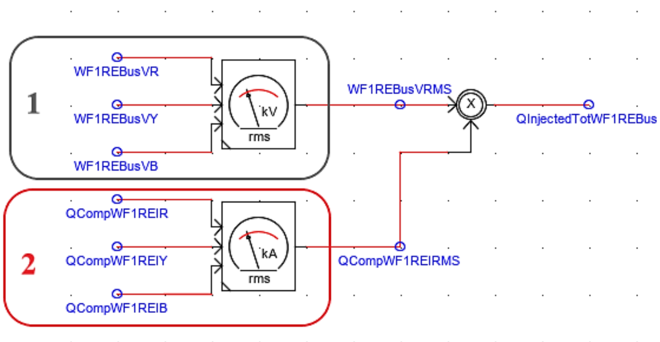

Figure 25. Monitoring and calculation logic for reactive power injection device using the RMS voltage and current.

Zone 1 shows the logic to calculate the RMS voltage from the busbar at which the reactive power compensator devices are connected. Also, in Zone 2, another RMS current calculator logic is shown and monitors the total line current drawn by the active capacitor bank unit. The RMS output from both zones is multiplied and the product gives the total reactive power injected.

The sequence switching of the capacitors for the reactive power compensator device is achieved by the logic shown in Figure 26. Similar logic is applied to the rest of the capacitors.

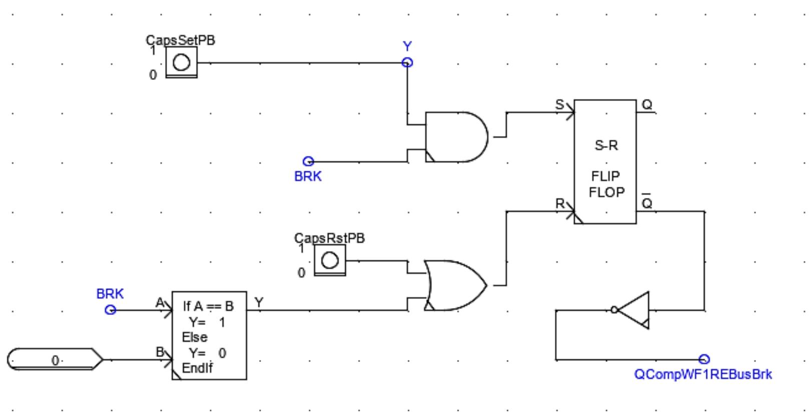

Figure 26. Monitoring and calculation logic for reactive power injection device switching logic.

4. Results

Under this test, the power flow was conducted and the aerodynamic, mechanical, and electrical quantities were monitored.

The operating temperature range for this wind turbine is from −20 °C to 45 °C, the test is carried out at a temperature of 25 °C. For as long as the temperature is within the specified operating range, the output power of the turbine may still be tuned to the desired output. Humidity and air pressure also play a role in the value of C_P and are set to 30% and 1415 mbar. The mechanical and electrical quantities were monitored during the steady-state operation of the wind power plant and at least one of the wind turbine generator unit results is shown in Table 6.

Table 6. Wind turbine generator unit monitoring at steady-state power flow.

Type of Data	Quantity	Values
Mechanical data	Wind speed	14 m/s
	Wind power	23.31 MW
	Wind turbine C_P	0.1718
	Wind turbine power	4.003 MW
	Wind turbine rotor speed	9.9 rpm
	Wind turbine torque	3.858 MN·m
Electrical data	WTGSU primary current	0.01563 kA
	WTGSU secondary current	0.00130 kA
	WTGU electrical torque	0.00986 PU
	WTGU terminal voltage	1.083 PU
	WTGU exciter reactive power	2.122 MVAr
	WTGU active power (P) output	0.02404 MW
	WTGU reactive power (Q) output	−2.010 MVAr
	WTGU reactive power circuit current	0.1633 kA

Monitored mechanical and electrical quantities for a single wind turbine generator unit (WTGU) at the steady-state power flow.

5. Discussions

The grid codes specify the continuous operating per-unit voltage level for Category C renewable power plants as 0.9 (minimum) to 1.0985 (maximum). As can be seen in Table 7, under normal load flow conditions, the voltage measured on the high-voltage busbar of the modeled wind power plant (WPP) is at 1.086 per unit, therefore acceptable.

Table 7. Wind power plant sending-end monitored values at the steady-state power flow.

Parameter	Actual Values	Per Unit Values
Group 1 collector terminal voltage	26.02 kV	1.084 PU
Wind farm sending-end bus voltage	249.9 kV	1.086 PU
Wind farm receiving-end bus voltage	249.9 kV	1.086 PU
Wind farm sending-end frequency	50 Hz	-
Wind farm receiving-end frequency	50 Hz	-

The wind power plant sending end and the receiving end terminal electrical quantities under steady-state power flow.

Another quantity specified by the grid codes is the operating frequency of a renewable power plant (RPP). It is stated that the RPP can be allowed to run continuously at the frequency range between 49 Hz to 51 Hz. The frequency of the modeled WPP does not violate the continuous operating range specified by the grid codes, as it is at 50 Hz under normal operating conditions. This means that the modeling and simulation (test) of the WPP model in this study are successful.

6. Conclusions

Modeling of a complete wind power plant (WPP) is presented in this article. The load flow of the wind power plant is carried out with the aim of the grid compliance test. Under this test, the mechanical and electrical quantities are monitored while the wind power plant is operated at a steady state. In terms of the grid compliance test, the electrical quantities are monitored at the sending and the receiving end terminals, since the WPP model consists of a transmission line system. The results show that the WPP operation complies with the grid codes, and can be integrated into the transmission power grid to conduct other studies such as voltage or frequency stability studies. Moreover, the WPP can be used by other scholars for testing various control methods for WPPs.

Author Contributions: Methodology, S.N.; Software, S.N.; Formal analysis, S.N.; Investigation, S.N.; Resources, A.K.R.; Data curation, S.N.; Writing—original draft, S.N.; Supervision, M.E.S.M.; Funding acquisition, M.E.S.M. and A.K.R. All authors have read and agreed to the published version of the manuscript.

Funding: This research received no external funding.

Data Availability Statement: Data and functional details presented in this study are available on request from the corresponding author.

Acknowledgments: Without the presence of the Center for Substation Automation and Energy Management Systems (CSAEMS), this research would not have been possible. Their facilities played a big role.

Conflicts of Interest: The authors declare no conflict of interest.

References

1. Ahmed, S.D.; Al-Ismail, F.S.M.; Shafiullah, M.; Al-Sulaiman, F.A.; El-Amin, I.M. Grid Integration Challenges of Wind Energy: A Review. *IEEE Access* **2020**, *8*, 10857–10878. [CrossRef]
2. Osman, A.M.; Alsokhiry, F. Sliding Mode Control for Grid Integration of Wind Power System Based on Direct Drive PMSG. *IEEE Access* **2022**, *10*, 26567–26579. [CrossRef]
3. Liu, M.; Pan, W.; Zhang, Y.; Zhao, K.; Zhang, S.; Liu, T. A Dynamic Equivalent Model for DFIG-Based Wind Farms. *IEEE Access* **2019**, *7*, 74931–74940. [CrossRef]
4. Nomandela, S.; Ratshitanga, M.; Elvis, M. IEC 61850 Standard-Based Protection of the Coupling Point between a Wind Farm and the Power Grid. Cape Peninsula University of Technology (CPUT). 2021. Available online: http://ir.cput.ac.za/handle/20.500.11838/3424 (accessed on 7 February 2022).

5. Hasnaoui, O.; Allagui, M. Dynamic performance improvement of wind farms equipped with three SCIG generators using STATCOM. *J. Energy S. Afr.* **2014**, *25*, 128–135. [CrossRef]
6. Rana, V.; Gupta, R.; Kumar, N. Integration of Wind Farm into a Weak Distribution Network. *Change* **2014**, *4*, 404–409.
7. Kim, C.; Dinh, M.-C.; Sung, H.-J.; Kim, K.-H.; Choi, J.-H.; Graber, L.; Yu, I.-K.; Park, M. Design, Implementation, and Evaluation of an Output Prediction Model of the 10 MW Floating Offshore Wind Turbine for a Digital Twin. *Energies* **2022**, *15*, 6329. [CrossRef]
8. Vilmann, B.; Randewijk, P.J.; Hjerrild, J.; Khalil, A. Frequency and Voltage Compliance Capabilities of Grid-Forming Wind Turbines in Offshore Wind Farms in Weak AC Grids. *Electronics* **2023**, *12*, 1114. [CrossRef]
9. Li, W.; Chao, P.; Liang, X.; Ma, J.; Xu, D.; Jin, X. A Practical Equivalent Method for DFIG Wind Farms. *IEEE Trans. Sustain. Energy* **2018**, *9*, 610–620. [CrossRef]
10. Zhang, Z.; Zhou, M.; Wu, Z.; Liu, S.; Guo, Z.; Li, G. A Frequency Security Constrained Scheduling Approach Considering Wind Farm Providing Frequency Support and Reserve. *IEEE Trans. Sustain. Energy* **2022**, *13*, 1086–1100. [CrossRef]
11. Liu, B.; Li, Z.; Wang, H.; Dong, X.; Su, W.; Li, G.; Chen, X.; Fernando, T.; Lu, H.H.C.; Lian, X.; et al. Impedance Modeling of DFIG Wind Farms with Various Rotor Speeds and Frequency Coupling. *IEEE Trans. Circuits Syst. II Express Briefs* **2021**, *68*, 406–410. [CrossRef]
12. Zhou, Y.; Zhao, L.; Hsieh, T.Y.; Lee, W.J. A Multistage Dynamic Equivalent Modeling of a Wind Farm for the Smart Grid Development. *IEEE Trans. Ind. Appl.* **2019**, *55*, 4451–4461. [CrossRef]
13. Castro, L.M.; Acha, E. On the Dynamic Modeling of Marine VSC-HVDC Power Grids including Offshore Wind Farms. *IEEE Trans. Sustain. Energy* **2020**, *11*, 2889–2900. [CrossRef]
14. Niwas, S.; Singh, S.N.; Ostergaard, J.; Jain, N. Distributed Generation in Power Systems: An Overview and Key Issues. *Citation*. 2009. Available online: http://orbit.dtu.dk/files/5202512/24IEC_paper.pdf (accessed on 18 April 2020).
15. Masters, G.M. *Renewable and Efficient Electric Power Systems*; Wiley and Sons: Hoboken, NJ, USA, 2004. [CrossRef]
16. Manwell, J.F.; McGowan, J.G.; Rogers, A.L. *Wind Energy Explained: Theory, Design, and Application*; Wiley and Sons: Hoboken, NJ, USA, 2010.
17. Burton, T.; Sharpe, D.; Jenkins, N.; Bossanyi, E. *Wind Energy: Handbook*; Wiley and Sons: New Delhi, India, 2011.
18. Zhang, X.; Wang, W.; Li, F.; Dai, Y. Individual pitch control based on fuzzy PI used in variable speed wind turbine. In Proceedings of the 2012 12th International Conference on Control Automation Robotics & Vision (ICARCV), Guangzhou, China, 5–7 December 2012; Volume 2012, pp. 1205–1208. [CrossRef]
19. Roussos, A.I.; Ntampasi, V.E.; Kosmidou, O.I. Pitch Control for Variable Speed Wind Turbines. In Proceedings of the 10th International Conference on Informatics in Control, Automation and Robotics, Reykjavík, Iceland, 29–31 July 2013; pp. 43–49. [CrossRef]
20. Dhar, M.K.; Ahmed, M.T.; Al, A. Study on Pitch Angle Control of a Variable Speed Wind Turbine using Different control strategies. In Proceedings of the 2017 IEEE International Conference on Power, Control, Signals and Instrumentation Engineering (ICPCSI), Chennai, India,, 21–22 September 2017; pp. 285–290.
21. Hwas, A.; Katebi, R. Wind turbine control using PI pitch angle controller. *IFAC Proc. Vol.* **2012**, *45*, 241–246. [CrossRef]
22. Jose, G.; Chacko, R. A review on wind turbine transformers. In Proceedings of the 2014 Annual International Conference on Emerging Research Areas: Magnetics, Machines and Drives (AICERA/iCMMD), Kottayam, India, 24–26 July 2014. [CrossRef]